

Ultra long period Cepheid H 42 in M 31

N. Taneva¹, A. Valcheva¹, G. P. Petrov¹, P. Nedialkov¹
Department Astronomy, Sofia University "St. Kl. Ohridski", BG-1164, Sofia
valcheva@phys.uni-sofia.bg

(Submitted on 06.12.2019. Accepted on 14.02.2020)

Abstract. We present photometric study of the variable star H 42 located in the stellar complex OB81 in M 31. We redetermine its period using archive *R*-band Palomar Transient Factory (PTF) data and find 177.32 ± 0.12 days. Phase curve analysis of these shows no period change in the time interval 2009–2015. When previous epochs data are taken into account, the analysis of the phase curves indicates that the period of H 42 is increasing, which is clearly seen in the O-C diagram. By the use of recent BVR photometry from Rozhen we calculated the extinction along the sight-line of H 42 in order to check the evolutionary status of H 42 on HR diagram. According to its position on the HR diagram, H 42 has a mass of $\sim 20 M_{\odot}$ and mean spectral class G0I. The period–luminosity diagram shows that H 42 obeys the linear relationship between *P* and Wasenheit magnitude, typical for Cepheids pulsating in the fundamental mode and is a promising distance indicator.

Key words: galaxies: individual (M 31) – stars: variables: Cepheids – stars: variables: individual (H 42) – extinction

Introduction

The classical Cepheids are a well known class of pulsating stars which populate the upper part of the instability strip in the Hertzsprung–Russell (HR) diagram. Generally, they have pulsation periods between 1 and 50 days. In 1929, Edwin Hubble discovered H 42 (J003953.55+402827.7) a variable in M 31 galaxy with period $P = 175$ days, and classified it as a Cepheid (Hubble 1929). Several decades later, Baade and Swope 1963 observed the same object and found a period of 176.7 days but doubted its Cepheid nature. The light curve of H 42 showed some changes from cycle to cycle and the authors suggested that the star is too bright in B-band for a long-period variable (LPV) in M 31. They rejected the possibility H 42 to be a faint LPV in our galaxy and emphasized its untypical red color. Sharov & Kholopov 1979 confirmed the changing shape of the light curve using new photographic photometry and determined the period of 176.6 days. They discussed the rare nature of Cepheids with very long periods and the lack of such stars in the Galaxy. Yet there are examples in other galaxies like HV 1956 a variable in the Small Magellanic Cloud (SMC) with a period of 210 days. Ivanov & Kurtev 1985 confirmed the period of 176.7 days for H 42. Although its light curve showed some irregularities, they speculated that the star is a Cepheid-like semiregular based on its luminosity which obeys the period-luminosity relation. Welch et al. 1986 published the first *H*-band infrared photometry of H 42. They had only seven epochs of observations and it was insufficient to estimate the period of the star, but they noted an unusually large brightness amplitude in *H*-band. The authors concluded that H 42 is probably not a Cepheid in the classical sense. A few decades later some authors proposed the idea that an individual class of “ultra-long period Cepheids” (ULPCs) with periods longer than 80 days and masses of about 15 – 20 M_{\odot} exists (Bird et al. 2009; Fiorentino et al. 2012). Using

data from the Palomar Transient Factory (PTF), Ngeow et al. 2015 identified two ULPC candidates in M31 and concluded that they are not usable standard candles.

On the other hand, Drout et al. 2009 studied yellow supergiants (YSGs) in M31 and their location in HR diagram to test the stellar evolution theory and classified H 42 as YSG, but did not discuss its variability. Gordon et al. 2016 spectroscopically confirmed 75 YSG in M31 and classified H 42 as G5I star. Recently, Soraisam et al. 2019, using data from intermediate PTF, studied the variability of around 500 massive stars in M31. They confirmed H 42 as YGS and reported a period of 170 days.

In this paper we present optical photometric study of H 42 - the ULPC in M31 galaxy. The paper is organized as follows. In Sect. 1, we describe the observational data - present-day and archive - used in this study. In Sect. 2, the light curve of H 42 and period search are discussed. The O-C diagram is presented therein. Sect. 3 is devoted to the evolutionary status of H 42 and our results are discussed in Sect. 4.

1. Observational data

Nowadays, the Palomar Transient Factory (PTF, Law et al. 2009) and the intermediate PTF (iPTF) robotic surveys offer multi-epoch Sloan g -band and Mould R -band¹ (hereafter r to avoid confusion with standard R) observations that are very suitable for studying long period variables. H 42 has been identified in the PTF catalog with good time coverage and gr band magnitudes were extracted. Information on the used PTF observational data is summarized in Table 1.

Table 1. Available observational data of H 42. PH stands for photographic magnitude and r for PTF Mould R magnitude.

Source Data	Time span	Band	# of points	P[days]	Ref
Hubble	1924 Sep - 1928 Aug	PH	55	175	Hubble 1929
Baade & Swope	1950 Aug - 1951 Dec	PH	53	176.7	Baade & Swope 1963
Sharov & Kholopov	1968 Aug - 1978 Jan	PH	41	176.6	Sharov & Kholopov 1979
PTF/iPTF	2009 Aug - 2015 Jan	r	1672	–	Law et al. 2009
PTF/iPTF	2011 Jan - 2014 Oct	g	120	–	Law et al. 2009

In late 2018 and 2019, photometric observations of H 42 were carried out with the 50/70 cm Schmid telescope at NAO Rozhen, Bulgaria. During the observations, the telescope was equipped with two different – 4kx4k FLI PL16803 and 4kx4k Andor – CCD cameras with a scale of $1.07''/pix$ and field of view of $73' \times 73'$. The stellar complex OB81, which contains the variable H 42 was positioned close to the center of the image to minimize variations in the PSF. The typical acquisition of the images in each filter was 300 sec. The obtained BVR-band frames were dark-field subtracted

¹ The PTF Mould R filter is very similar in shape to the SDSS r -band filter, but shifted 27 \AA redwards

Table 2. BVR photometric data of H 42 from 50/70 cm Schmidt telescope at NAO Rozhen, Bulgaria.

Date	JD2400000	B	σ B	V	σ V	R	σ R	Phase
yyyy/mm/dd	[days]	[mag]	[mag]	[mag]	[mag]	[mag]	[mag]	
2018/10/02	58394.42153	18.547	0.031	17.544	0.022	16.966	0.018	0.841
2018/10/04	58396.40972	18.671	0.040	17.533	0.024	16.964	0.018	0.853
2018/10/05	58397.38958	18.595	0.033			16.946	0.023	0.858
2018/10/06	58398.38889	18.597	0.039	17.488	0.024	16.938	0.017	0.864
2018/11/11	58434.32292	19.109	0.081	17.765	0.027	17.091	0.016	0.066
2018/12/02	58455.33264	19.689	0.055			17.314	0.028	0.185
2019/07/06	58671.49958					17.440	0.022	0.404
2019/07/08	58673.48777	19.863	0.126			17.446	0.027	0.415
2019/08/28	58724.50376	19.154	0.066			17.329	0.022	0.703
2019/09/27	58756.44998	18.586	0.036	17.539	0.019	16.840	0.017	0.883
2019/10/26	58783.36165	19.034	0.046	17.607	0.017	16.853	0.014	0.035
2019/10/27	58784.21299	19.102	0.055	17.563	0.018	16.880	0.015	0.040

and flatfielded and the final image is a result from 3x300/5x300 sec co-added frames. For this study only the central 15'x15' field, containing OB81, was considered. Since H 42 is a part of the latter stellar complex and the crowding is sufficient, we performed PSF photometry using standard IRAF² routines. For standard BVR magnitude calibration we used between 30 and 35 stars from the LGGs (Massey et al. 2016). The obtained BVR-band magnitudes for H 42 are presented in Table 2.

To analyze the long term photometric behavior of H 42, we searched for well-sampled archive data with more than 40 data points. Since H 42 is quite bright star, with $V < 18$ mag in M 31, it was first discovered by Hubble 1929 who presented its first photographic series. Further, we found data on H 42 in two other comprehensive photographic studies - Baade & Swope 1963 and Sharov & Kholopov 1979. A brief information on these data sets is presented in Table 1.

2. Light curve analysis

2.1 Light curve

PTF *gr* photometric data were extracted and used to construct the H 42 light curve (see Fig. 1). Five cycles in *r*-band light curve are well outlined and allow us to study the photometric behavior of H 42. It is clearly visible that the first minimum is nearly 0.4 mag deeper than the others, which indicates significant amplitude decrease within time scale of two cycles. This peculiarity is not repeatable in the available data. Unfortunately, *g*-band data are sparse, parts of only three cycles are observed and data points are missing in the time of the first detected *r* minimum.

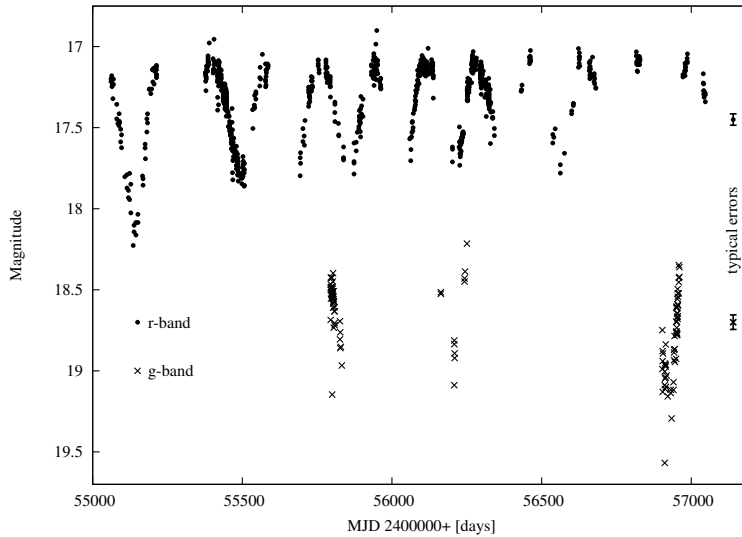


Fig. 1. PTF light curve of H 42, where dots and crosses represent r and g -band magnitudes, respectively. Typical errors are shown on the right.

2.2 Period search

Since we have multi-epoch data from PTF, we carried out period search using the interactive fitting tool Exo-Striker³ (Trifonov 2019) which uses Lomb–Scargle algorithm for searching for periodic signals in the data. We used all available data and searched in large interval across period. The most probable period is the one corresponding to the highest peak in the periodogram. The peak in the power spectrum of H 42 r -band data gives $P=177.32 \pm 0.12$ days with 0.86 level of significance. This period is adopted and used to construct the folded light curves with the ephemeris $MJD = 2455052.98 + 177.32E$ based on different data sets. The initial moment was chosen so that the moment of minimum light coincides with $\varphi=0.5$. The light curves are plotted in chronological order in Fig. 3, starting with Hubble data (pluses), followed by Baade & Swope data (open triangles), Sharov & Kholopov 1979 (open circles) and PTF rg data (dots and crosses, respectively). To separate the curves, different constants were added to the magnitudes (see the label of Fig. 3). Rozhen R magnitudes, transformed (see Sect.) into r PTF magnitudes, are overplotted in the r PTF folded light curve with open squares. As can be seen in the latter figure, H 42 curves exhibits the characteristic shape with slow decline and quick rise in

² IRAF is distributed by the National Optical Astronomy Observatories, which are operated by the Association of Universities for Research in Astronomy, Inc., under cooperative agreement with the National Science Foundation.

³ <https://ascl.net/1906.004>

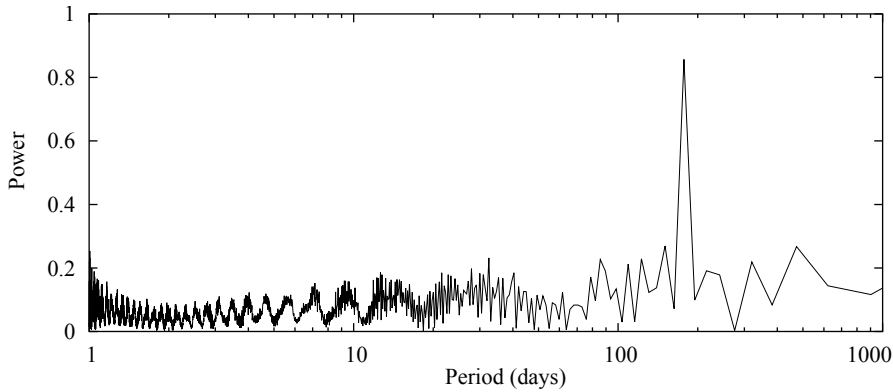


Fig. 2. Power spectrum of H 42 PTF data obtained with *Exo-Striker* (Trifonov 2019). The peak corresponds to $P=177.32$ days.

the bluer pass-bands but the phase of the minimum light is shifted for the different epoch series.

2.3 O-C diagram

(O-C) diagrams are powerful tools for finding period changes. We assume that H 42 pulsated with a constant period within the time span of each data set. Applying the same period search tool (see Sect.) we obtained $P = 177.2 \pm 1.7$ days for Hubble 1929, $P = 177.5 \pm 2.0$ days for Baade and Swope 1963 and $P = 178.7 \pm 0.8$ days for Sharov & Kholopov 1979. Let us note that the Sharov & Kholopov 1979 ephemeris $JD_{max} = 2429550.820 + 176.55E$ was determined by combining data from different epochs, something that has been avoided in this study.

As clearly seen in Fig.3 there is a phase shift $\Delta\varphi$ between the light curves from Table 1 and the PTF light curve, all constructed for one and the same period of 177.32 days. We interpreted that shift as a proof for a slow period change and calculated (O-C) as $P\Delta\varphi$ by fitting the minimum of each data set independently. Most of the (O-C) error comes from the error of $\Delta\varphi$, which is typically ~ 0.05 . Unfortunately, the data set of Sharov & Kholopov 1979 has very poor coverage at minimum light and no fitting is possible. In fact, it is only one unique point which we assume to coincide with the minimum light of H 42 but with a much higher $\Delta\varphi$ uncertainty, equal to 0.15.

We plotted in Fig.4 all derived (O-C) with x-axis error bars representing the time span of each data set (see Table 1). There are clear indications that the period of H 42 may have increased during the time span of all observations with ~ 0.8 day per century (if Sharov & Kholopov 1979 data are not taken into account), or it initially increased at higher speed of ~ 1.4 day/century until mid 70's of the last century and later on stabilized.

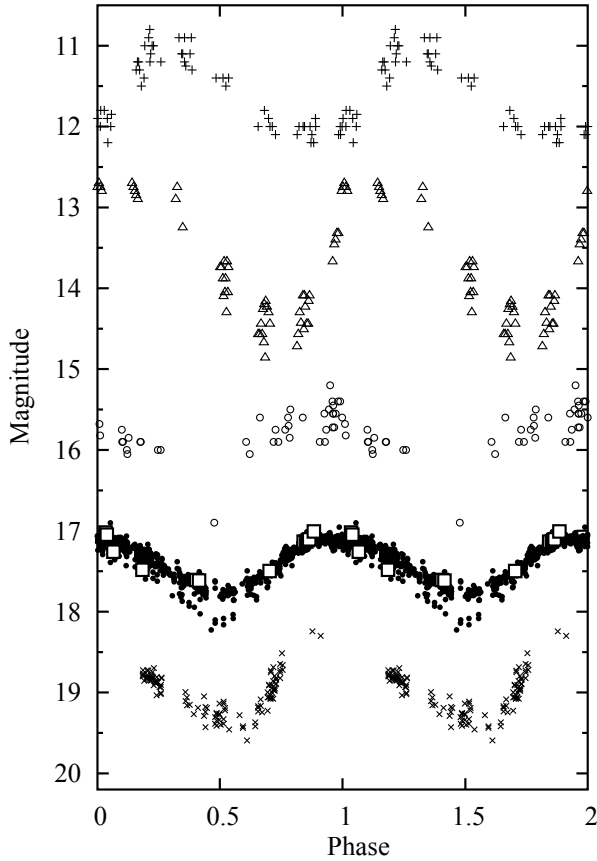


Fig. 3. Folded light curves of H 42 constructed using the different data sets. Photographic magnitudes from Hubble 1929 (pluses) are shifted in Y axis with -7 mag, from Baade & Swope 1963 (open triangles) with -5.5 mag, and from Sharov & Kholopov 1979 with -3.8 in order to avoid overlapping. PTF *gr* data are shown with crosses and dots, respectively, and g-band magnitudes are shifted with $+0.3$ mag. R data from NAO Rozhen (Table 2) were transformed in the PTF system (see Sect.) and shown with open squares. All curves were calculated with the period which corresponds to the peak of the power spectrum $P=177.32$ days and unique initial moment.

3. HRD and P–L diagnostic

In order to check the evolutionary status of H 42 on the HR diagram, we determined its effective temperature and bolometric luminosity from the medians over the PTF *gr* light curves and its median Rozhen B magnitude and $(B-R)$ color, as described below.

We approximated the zero-reddening line of Bessell 1990 for supergiants with 7 observational points from the Rozhen data (see Table 2) and the available $(B-V)$ and $(B-R)$ colors by varying the amount of the extinction correction $E(B-V)$ and assuming Cardelli et al. 1989 extinction curve with

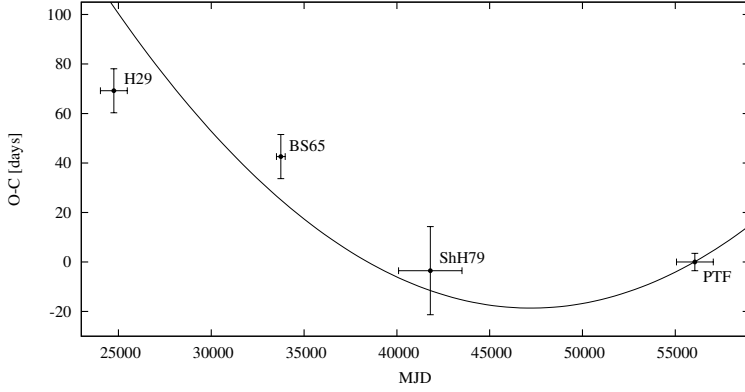


Fig. 4. (O-C) diagram of H 42 within the observed r-band light curve minima.

$R_V=3.1$. Our best fit estimate is $E(B - V) = 0.57 \pm 0.05$ which is almost twice as large as the $E(B - V) = 0.34$ mag, adopted by Gordon et al. 2016. Thereafter we applied everywhere absorption $A_B = 2.34 \pm 0.22$ and reddening correction $E(B - R) = 0.88 \pm 0.08$.

Bolometric correction and temperature are determined by the use of Flower 1996 transformations for intermediate-type supergiants. The adopted distance modulus of 24.4 ± 0.1 mag is taken from van den Bergh (2000).

The H 42 median $r = 17.41$ mag and $g = 18.56$ mag were converted into standard V and $(B - V)$ by the use of the following transforming equations:

$$\langle g \rangle - \langle r \rangle = -0.236 + 0.88(B - V) + 0.130(B - V)^2 \quad (1)$$

$$V - \langle g \rangle = 0.178 - 0.423(B - V) - 0.01(B - V)^2 \quad (2)$$

$$R - \langle r \rangle = -0.191 + 0.153(B - V) - 0.125(B - V)^2 \quad (3)$$

where $\langle g \rangle$ and $\langle r \rangle$ are the average PTF magnitudes of 287 stars in common with stars from LGGs and with more than 1000 detections in r -band and more than 30 detections in g -band. The transformation equations are visualized in Fig. 6 by plotting the differences against the $(B - V)$ color.

This results in $V = 18.16$ mag and $(B - V) = 1.32$ mag. After applying the proper correction for extinction, we put the PTF data point on the HR diagram. Considering the stellar evolutionary tracks, accounting for the effects of rotation and using solar metallicity $z = 0.014$ (Ekström et al. 2012), we estimated a mass of $\sim 20 M_\odot$ for H 42 (see Fig. 5). Most recently,

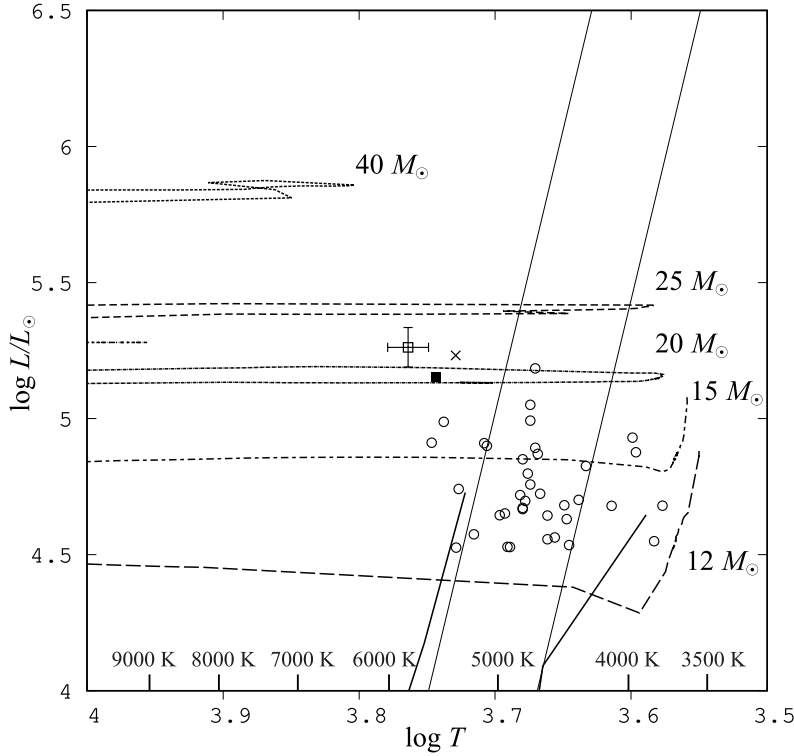


Fig. 5. H 42 location in the HRD diagram. The filled square shows the adopted value of $\log T$ and $\log L/L_{\odot}$ based on the median PTF rg light curve magnitudes. The value based on median Rozhen BR magnitudes is plotted with an open square and the one proposed by Gordon et al. 2016 is plotted with an X. The locations of 37 ultra-long (period between 80–210 days) Cepheids in nearby galaxies from the lists of Bird et al. 2009 and Fiorentino et al. 2012 are shown with open circles. Dashed lines denote the stellar evolutionary tracks, accounting the effects of rotation and solar metallicity $z = 0.014$ (Ekström et al. 2012). The boundaries of the classical instability strip are presented with straight lines (Tammann et al. 2003), as well as model boundaries of Anderson et al. 2016 for fundamental mode and $z = 0.014$.

the location of H 42 was given by Gordon et al. 2016. Their estimate is based on both tight $V=17.451 \pm 0.004$ mag and color $(B - V)=1.184 \pm 0.004$ mag from Massey et al. 2016 averaged over 10 observations done during maximum light. Interestingly, Gordon et al. 2016 classified H 42 as a G5 supergiant according to its spectrum (Martin et al. 2017), obtained near minimum light at phase $\varphi=0.595$ (blue arm) and $\varphi=0.507$ (red arm). Note that combining lesser reddening correction with brighter apparent magnitude results in luminosity similar to our luminosity estimate.

Another independent location of H 42 on the HR diagram is obtained by the means of the median value $B = 19.03$ mag and $(B - R) = 1.82$ over 11 observational points from the Rozhen data (see Table 2). We plotted it with error bars typical for a single observational point. The two obtained

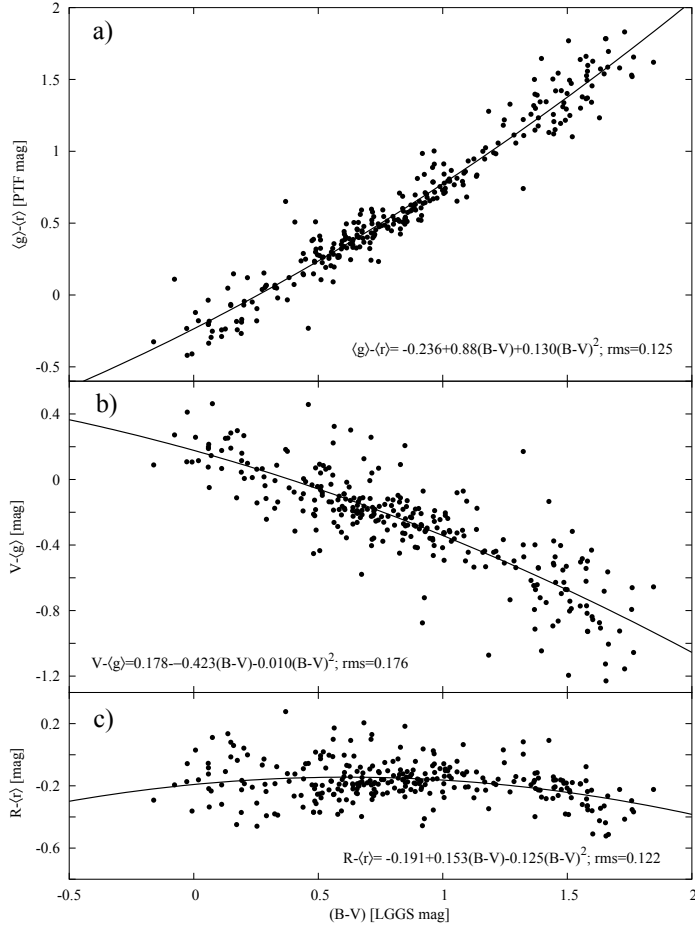


Fig. 6. 287 objects with more than 1000 observations in r and 30 observations in g -band from PTF, cross-identified with BVR photometry of Massey et al. 2016 in $15' \times 15'$ field containing OB 81. For each filter in PTF, average magnitude of all observations is taken into account. The coefficients of the fitting parabolas are shown in the figure.

positions of H 42 on the HR diagram are in a good agreement and the difference can be explained with the fact that most Rozhen observations were taken close to the maximum light.

Cepheids obey a period–luminosity relation and it is interesting to see if H 42 follows it. Instead of luminosity, we used reddening-free Wesenheit magnitude W_{gr} defined as: $W_{gr} = g - R_{gr}(g - r)$, where R_{gr} is defined as: $R_{gr} = A_g / (A_g - A_r)$. Its value $R_{gr} = 3.38$ is calculated again from the standard extinction curves (Cardelli et al. 1989) with $R = 3.1$. In Fig. 7 the constructed Period–Wesenheit relation based on M 31 Cepheids data from The PAndromeda Cepheid Sample catalog of Kodric et al. 2018 is shown. The sample contains 737 Cepheids with available gr photometry

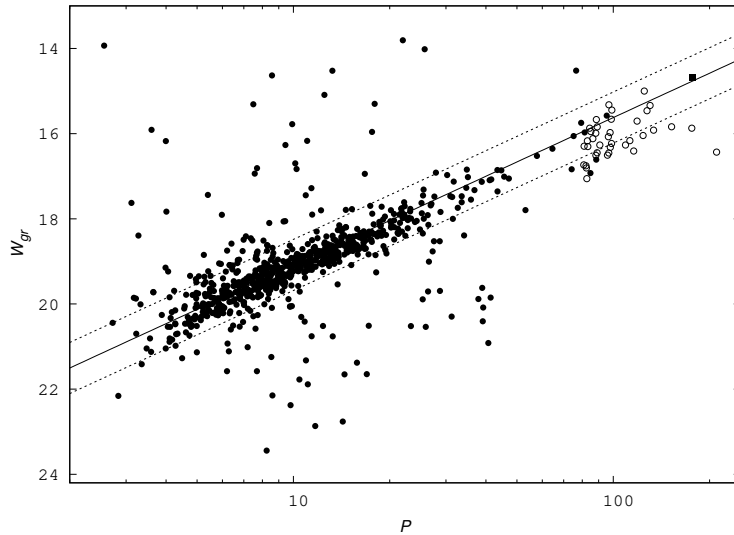


Fig. 7. Period–Wesenheit relation for the fundamental mode based on the Cepheid sample from Kodric et al. 2018 (filled circles). 37 ULP Cepheids from the lists of Bird et al. 2009 and Fiorentino et al. 2012 are shown with open circles. H 42 is marked with filled square (see Sect.). The dashed lines denote 3σ deviations.

(here we neglect the small differences between PanStarrs and PTF magnitudes) pulsating in fundamental mode with period error less than 0.1 day and Wesenheit index error less than 0.1 mag. It was found that 591 ($\sim 80\%$) of them obey the linear relationship with standard deviation $\sigma=0.1$ mag. For completeness we added 37 ultra-long Cepheids from the lists of Bird et al. 2009 and Fiorentino et al. 2012.

We calculated the Wesenheit magnitude of H 42 for $r = 17.41$ mag and $g = 18.56$ mag median over the light curve magnitudes and found that it is well within the 3σ boundaries of the linear fit and deviates only 0.4σ .

4. Discussion

It is well known that the mean spectral type of Cepheids varies with luminosity (Tammann et al. 2003) and the expected temperature at the middle of the instability strip for luminosity $\log L/L_{\odot} \sim 5.3$, according to the Flower 1996, is $\log T \sim 3.65$, typical for late spectral class G8I. Note that the H 42 HR estimates, based on both Rozhen and PTF data, varied in the spectral range F5I–G5I, consistent with the spectral G5I detection of Martin et al. 2017 at the minimum light. Since the true location of the instability strip remains rather uncertain for $\log L/L_{\odot} > 4.7$, we determined the temperature and the luminosity for a sample of 37 ultra-long (period between 80–210 days) Cepheids in nearby galaxies taken from the lists of Bird et al. 2009 and Fiorentino et al. 2012 and added them in Fig. 5, where there are

some indications that the instability strip may get broader at higher luminosities. H 42 is positioned on the left side of the instability strip crossed twice by the evolutionary track of $20 M_{\odot}$ (Ekström et al. 2012). Since the period of the variable is increasing, one could associate this with the first crossing of the instability strip when the star evolves towards its cool edge (Turner et al. 2006). The ultra-long period of 177.32 days itself may be due to the location of the variable outside the instability strip, but also driving mechanisms other than the radial pulsations may act. In a forthcoming paper we will focus on the changing spectrum of H 42 as their indicator.

Nevertheless, the variations of the amplitude and phase of maximum seen in the light curve of H 42 (see Fig. 3) as a function of increasing wavelength follows the typical behavior of Cepheid pulsating in the fundamental radial mode (Madore & Freedman 1991, Catelan & Smith 2015) and characterized by monotonic drop in amplitude, the progression toward more symmetric light variation, and the phase shift of maximum toward later phases, all with increasing wavelength. The well defined amplitudes of H 42 are $\Delta A_B=1.31$, $\Delta g=1.15$ mag $\Delta A_r=1.05$ and $\Delta A_R=0.62$, but note that $\langle \Delta A_r \rangle=0.65$ during the consecutive minima in the PTF r -band light curve (see Fig. 1 and Fig. 3). The r PTF photometry shows that, while H 42 period stays stable, the light amplitude variations may be in progress. In that sense H 42 is not a unique ULPC. The SMC variable HV1956, with period of 210.4 days (Bird et al. 2009), also has significant amplitude changes in the light curve. However, none of the other 36 ULPCs from Bird et al. 2009 and Fiorentino et al. 2012 presents significant amplitude changes. Thus, we cannot generalize that the amplitude changes are typical for the ULPCs as they are for the low-amplitude and short period Cepheids (e.g. Polaris, Brown & Bochonko 1994). We exclude that H 42 could be a semiregular red star and explain its red color as a result of higher absorption $A_B=2.3$, still consistent with the total $N(H)$ column density (Braun et al. 2009) indicating maximum $A_B=2.9$ along that sight line. Taking also into account that H 42 follows the P–L relation for M 31 Cepheid sample of Kodric et al. 2018, it is most likely a Cepheid variable. The same conclusion is confirmed also by the sample of 37 ultra-long Cepheids (Bird et al. 2009 and Fiorentino et al. 2012) in nearby galaxies, although more precise analysis is needed.

Conclusions

We derive a new period of 177.32 ± 0.12 days of the variable H 42 in the stellar complex OB81 in M 31 using multi-epoch gr photometry and original BVR photometry from NAO Rozhen. It is interesting to note that the first minimum in PTF light curve is deeper than other registered ones. This feature is observed only once in the constructed light curve.

The available BVR photometry allows us to estimate on the color-color $(B - V) - (B - R)$ diagram the extinction $A_B = 2.34 \pm 0.22$ towards H 42. This value is larger than the previous estimates but still consistent with the $N(H)$ column density (Braun et al. 2009) along that line of sight.

The position of H 42 in the HR diagram indicates a $\sim 20 M_{\odot}$ star evolving towards the cool edge of the instability strip, as testified by its increasing period. High luminosities and large amplitudes of all ultra-long Cepheids,

together with H42, make them promising distance indicators.

Acknowledgments: The authors gratefully acknowledge observing grant support from the Institute of Astronomy and National Astronomical Observatory, Bulgarian Academy of Sciences.

The authors thank the referee for his thoughtful comments which improve our work and Andon Kostov and Milen Minev for their contribution during the observational campaign.

This research has made use of the VizieR catalogue access tool, CDS, Strasbourg, France (DOI: 10.26093/cds/vizieer). The original description of the VizieR service was published in A&AS 143, 23.

The Intermediate Palomar Transient Factory project is a scientific collaboration among the California Institute of Technology, Los Alamos National Laboratory, the University of Wisconsin, Milwaukee, the Oskar Klein Center, the Weizmann Institute of Science, the TANGO Program of the University System of Taiwan, and the Kavli Institute for the Physics and Mathematics of the Universe.

This study was partially funded by the Science Fund of the Sofia University with grant N80-10-98/15.04.2019; National Science Fund of Bulgaria with grant DN18/10-11.12.2017 and Ministry of Education and Science of the Republic of Bulgaria, National RI Roadmap Project DOI-277/16.12.2019.

References

- Anderson R.I., Saio H., Ekström S., Georgy C., Meynet G., 2016, *A&A*, 591, A8
 Baade W. & Swope H.H., 1963, *AJ*, 68, 435
 Bird J.C., Stanek K.Z. & Prieto J.L., 2009, *ApJ*, 695, 874
 Bessell M. S., 1990, *PASP*, 102, 1181
 Braun R., Thilker D.A., Walterbos R.A.M., Corbelli E., 2009, *ApJ*, 695, 937
 Brown Ch. & Bochonko D. R., 1994, *PASP*, 106, 964-966
 Cardelli J.A., Clayton G.C., Mathis, J.S., 1989, *ApJ*, 345, 245
 Catelan M., Smith H. A., 2015, *Pulsating Stars*
 Drout M.R., Massey P., Meynet G., Tokarz S., Caldwell N., 2009, *ApJ*, 703, 441
 Ekström S., Georgy C., Eggenberger P., et al., 2012, *A&A*, 537, 146
 Fiorentino G., Clementini G., Marconi M., et al., 2012, *Ap&SS*, 341, 143
 Flower P. J., 1996, *ApJ*, 469, 355
 Gordon M.S., Humphreys R.M., and Jones T.J., 2016, *ApJ*, 825, 50
 Hubble E., 1929, *CMWCI*, 376, 1H
 Ivanov G.R. & Kourtev K., 1985, *Info. Bull. Variable Stars*, No. 2666
 Kodric M., Riffeser A., Hopp U. et al., 2018, *AJ*, 156, 130
 Law N.M., Kulkarni S.R., Dekany R.G. et al., 2009, *PASP*, 121, 1395
 Madore, B. & Freedman W., 1991, *PASP*, 103, 993
 Martin J.C. & Humphreys R.M., 2017, *AJ*, 154, 81
 Massey P., Neugent K.F., Smart B.M., 2016, *AJ*, 152, 62
 Ngeow C., Lee C., Yang M. T. et al., 2015, *AJ*, 149, 66
 Sharov A.S. & Kholopov P.N., 1979, *Promenyje Zvezdy*, 21, 219
 Soraisam, M. D., Bildsten, L., Drout, M. R. et al., 2019, *arXiv190802439*
 Tammann, G. A., Sandage, A., Reindl, B., 2003, *A&A*, 404, 423
 Trifonov, T. 2019, The Exo-Striker: Transit and radial velocity interactive fitting tool for orbital analysis and N-body simulations, <https://ascl.net/1906.004>
 Turner, G. A., Sandage, A., Reindl, B., 2003, *A&A*, 404, 423
 Welch D.L., McAlary C.W., McLaren R.A., Madore B.F., 1986, *ApJ*, 305, 583